

# Accuracy and Reliability in Differentiating Retinal Arteries and Veins Using Widefield En Face OCT Angiography

Akihiro Ishibazawa<sup>1,2</sup>, Nihaal Mehta<sup>1,3</sup>, Osama Sorour<sup>1,4</sup>, Phillip Braun<sup>1</sup>, Sarah Martin<sup>1</sup>, A. Yasin Alibhai<sup>1</sup>, Adnan Saifuddin<sup>1</sup>, Malvika Arya<sup>1</sup>, Caroline R. Baumal<sup>1</sup>, Jay S. Duker<sup>1</sup>, and Nadia K. Waheed<sup>1</sup>

<sup>1</sup> New England Eye Center, Tufts Medical Center, Boston, MA, USA

<sup>2</sup> Department of Ophthalmology, Asahikawa Medical University, Asahikawa, Japan

<sup>3</sup> The Warren Alpert Medical School of Brown University, Providence, RI, USA

<sup>4</sup> Department of Ophthalmology, Tanta University, Tanta, Egypt

**Correspondence:** Nadia K. Waheed, Tufts Medical Center, New England Eye Center, 800 Washington Street, Box 450, Boston, MA 02111, USA. e-mail: nwaheed@tuftsmedicalcenter.org

**Received:** 24 January 2019

**Accepted:** 7 April 2019

**Published:** 28 June 2019

**Keywords:** optical coherence tomography; retinal vasculature; image analysis; retina; diabetic retinopathy

**Citation:** Ishibazawa A, Mehta N, Sorour O, Braun P, Martin S, Alibhai AY, Saifuddin A, Arya M, Baumal CR, Duker JS, Waheed NK. Accuracy and reliability in differentiating retinal arteries and veins using widefield en face OCT angiography. *Trans Vis Sci Tech.* 2019;8(3):60, <https://doi.org/10.1167/tvst.8.3.60>

Copyright 2019 The Authors

**Purpose:** To evaluate the accuracy and reliability in differentiating retinal arteries from veins using widefield optical coherence tomography angiography (OCTA).

**Methods:** Ten healthy eyes and 12 eyes from diabetic patients were included. Foveal-centered swept-source OCTA images (12 × 12 mm) were obtained using the PLEX Elite 9000. Vessels were graded as arteries or veins by two independent, masked readers. Arteriovenous crossings were also evaluated in healthy eyes. The vessel identification gold standard was defined using color fundus photographs (CFP) for normal eyes and both CFP and fluorescein angiography for diabetic eyes. Grading accuracy was compared to the gold standard and reliability between readers assessed.

**Results:** The study evaluated 538 vessels (119 first order, 110 second, 309 third) in healthy eyes and 645 vessels (184 first order, 159 second, 302 third). In healthy eyes, the average accuracies identifying all, first-, second-, and third-order vessels were 98.61%, 99.16%, 100%, and 98.06%, respectively. Cohen's  $\kappa$  between graders in all vessels was 0.948. In diabetic eyes, the average accuracies identifying vessels were 96.90%, 99.46%, 97.77%, and 94.85%, respectively. Cohen's  $\kappa$  between graders for all vessels was 0.888. For crossing identification, the average accuracy and Cohen's  $\kappa$  were low (60.71% and 0.659, respectively).

**Conclusions:** En face OCTA allows for accurate and reliable artery and vein identification; for small branches and crossings, identification by en face OCTA alone may be less accurate and reliable.

**Translational Relevance:** Arteries and veins can be differentiated on OCTA, assisting in clinically identifying pathology as arterial or venous side.

## Introduction

The retina is the only organ in which arteries and veins can be directly observed. Assessment of retinal arteries and veins is an invaluable tool in gleaned clinically useful information for the diagnosis of not only ocular disorders but also systemic diseases. Examples of retinal changes in systemic disorders include focal arterial narrowing and arteriovenous nicking due to hypertensive and atherosclerotic

changes,<sup>1-3</sup> venous beading and tortuosity in diabetic retinopathy (DR), and vessel occlusions indicative of underlying vascular disease.<sup>4-6</sup> Largely for this reason, direct fundoscopic examination has historically been an important and commonly deployed diagnostic tool across medical fields. A number of studies performing artery-vein classification based on color fundus images have also demonstrated that quantitative metrics, such as the artery/vein vessel caliber and their caliber ratio can be useful in predicting systemic diseases.<sup>7-13</sup> This further demon-

strates the potential utility of direct in vivo visualization of retinal blood vessels.

Clinical adoption of optical coherence tomography (OCT) angiography (OCTA) has provided clinicians with a noninvasive, volumetric modality for visualizing the retinal vasculature at micrometer resolutions.<sup>14,15</sup> This method allows for easy assessment of not only precapillary arterial and venous changes but also capillary-level alterations, which is not possible using conventional vascular imaging modalities such as color fundus photography (CFP) or fluorescein angiography (FA). Critical to these assessments is the ability to accurately differentiate retinal arteries and veins in order to determine the location of vascular pathology. For instance, para-central acute middle maculopathy (PAMM) on the arterial side or in a globular pattern has been shown to be due to retinal artery occlusion,<sup>16,17</sup> whereas perivenular PAMM is related to retinal vein occlusion (RVO)<sup>16,18</sup>—diseases with distinct pathophysiologies, risk factors, and, potentially, management courses. Similarly, predominantly venous-side origins of neovascularization elsewhere (NVE) and intraretinal microvascular abnormalities (IRMAs) are associated with DR,<sup>19</sup> and venous-side collaterals with RVO.<sup>20</sup> Differentiating arteries from veins on retinal imaging is thus critical to accurate diagnosis and management. Alam et al.<sup>21</sup> recently demonstrated that color fundus image-guided artery-vein classification using OCTA images was an accurate method and showed improved sensitivity in OCTA-based detection and classification of DR. In recent studies, Balaratnasingam et al.<sup>22</sup> histologically showed the capillary-free zone (approximately 30–50  $\mu\text{m}$  in diameter) along parafoveal retinal arteries and also demonstrated that four different OCTA devices could clearly visualize this zone along retinal arteries but not veins. Muraoka et al.<sup>23</sup> also demonstrated that averaged high-resolution OCTA images enhanced visualization of the capillary-free zones around the arteries. These findings suggest one means by which arteries can be directly identified on OCTA alone.

However, no study has yet demonstrated whether OCTA images can be used on their own for accurate identification of arteries and veins as compared to conventional imaging. In this study, we evaluated the accuracy and reliability in differentiating arteries and veins using only widefield OCTA en face images as compared to identification using conventional imaging modalities.

## Methods

### Study Population

This cross-sectional observational study was approved by the Institutional Review Board (IRB) at Tufts Medical Center. The research adhered to the Declaration of Helsinki and the Health Insurance Portability and Accountability Act.

We prospectively recruited 10 healthy volunteers with no retinal pathology at the New England Eye Center (Boston, MA) between September and November 2018. Written informed consent was obtained in accordance with the Tufts Medical Center IRB. We also retrospectively identified patients with DR who had undergone CFP (Optos California; Optos PLC, Dunfermline, Scotland), FA (Optos California or Spectralis; Heidelberg Engineering, Heidelberg, Germany), and widefield OCTA imaging. DR was diagnosed and classified by two retina specialists (NKW and CRB) according to the International Clinical Diabetic Retinopathy Severity Scale.<sup>5</sup> We did not include eyes with severe media opacities, including severe cataract or vitreous hemorrhage, a history of vitrectomy, other chorioretinal disorders such as age-related macular degeneration, or primary retinal artery or vein occlusion.

### Image Acquisition

OCTA images were obtained using a swept-source OCTA instrument (PLEX Elite 9000; Carl Zeiss Meditec Inc., Dublin, CA) that operates at an A-scan rate of 100 kHz, with an axial resolution of 6.3  $\mu\text{m}$  and a transverse resolution of 20  $\mu\text{m}$ . OCTA volumes covering a 12  $\times$  12-mm retinal area (40° field of view) and centered at the fovea were acquired. Each 12  $\times$  12-mm volume consisted of 500 A-scans per B-scan and 500 B-scan locations per volume scan. Two repeated B-scans were obtained at each B-scan position to generate the OCTA images. En face OCTA images of the whole retina, generated by automatically segmenting the inner limiting membrane to 70  $\mu\text{m}$  above the retinal pigment epithelium, were exported for analysis. OCTA imaging was performed by trained ophthalmic photographers who repeated image acquisitions several times if necessary to ensure that images with good OCT signal penetration (signal strength  $\geq 7$ ) and minimal motion artifacts were obtained. This protocol is consistent with the standard imaging protocol at the New England Eye Center. In healthy subjects, CFPs

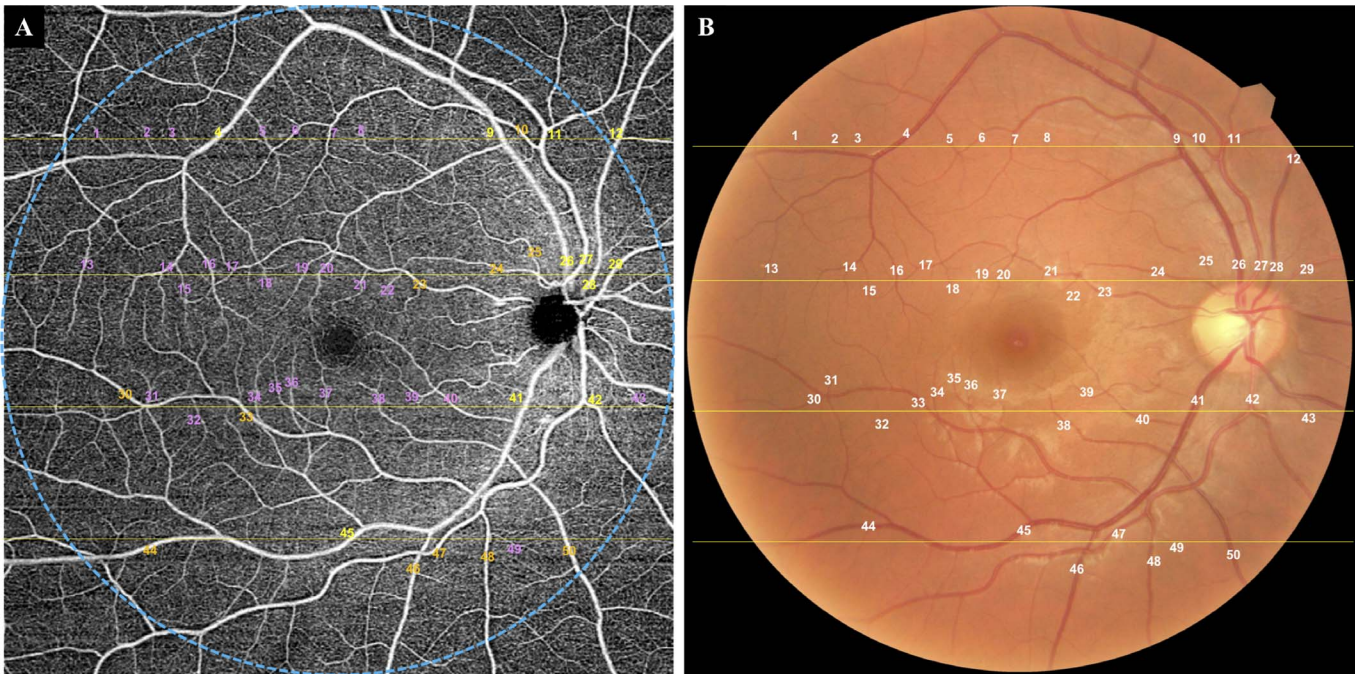


**Figure 1.** Objective determination of evaluated vessels in the en face OCTA image (A) and the CFP (B). (A) The  $12 \times 12$ -mm OCTA image of the right eye from a 30-year-old healthy male. The *blue-dot circle* represents the area covered by the CFP. Four *horizontal yellow lines* (every 2.4 mm) are placed on the image, and the vessels that intersect with the lines are evaluated as arteries or veins by independent masked readers. *Yellow, orange, and pink numbers* indicate first-, second-, and third-order vessels, respectively. (B) A high-resolution CFP used for making the gold standard vessel determination in the same eye as (A). The same four *horizontal yellow lines* (every 2.4 mm) are also placed on the image, and the vessels that intersect with the lines are evaluated as arteries or veins by retinal specialists.

centered on the fovea were also taken using a high-resolution (12-megapixel) nonmydriatic fundus camera equipped in a microperimeter (MP-3; NIDEK Co., Gamagori, Aichi, Japan).

### Identification of the Vessels as Arteries and Veins

To objectively determine which vessels would be evaluated, four horizontal lines (every 2.4 mm) were placed on the  $12 \times 12$ -mm OCTA images, and the vessels that intersected with the lines were designated for grading into arteries or veins (Fig. 1A). We included only first-, second-, and third-order vessels. Two masked readers independently performed grading on the en face OCTA images without seeing either the CFP or FA images from the other instruments. Prior to grading, the readers were trained by instructing them on the following rules: (1) The presence of surrounding hypointense areas, representing the capillary-free zone, are associated with arteries; (2) arteries do not cross other arteries and veins do not cross other veins, physiologically; (3)

vessels can be traced back proximally and distally to aid in identification.

The gold standard for vessel identification as arteries and veins, as well as the order of the vessels (e.g., first-versus second-order), was derived by two retinal specialists (OS and AI) using CFP for normal eyes (Fig. 1B) and both CFP and FA for diabetic eyes. Especially in the eyes with severe DR, differentiating retinal arterioles and venules using only CFPs is not guaranteed because retinal hemorrhages and exudates can conceal the small vessel branches. Moreover, the retinal arterioles sometimes become too sclerotic (i.e., hyalinized) to be identified on CFPs (Supplemental Fig. S1). Therefore, we used both CFP and FA for the gold standard in diabetic eyes. The same four horizontal lines that had been placed on the OCTA images were also placed on the CFP and FA images, and the vessels that intersected with the lines were likewise evaluated as arteries or veins. When discrepancies occurred between the results, they were openly discussed by the retinal specialists and a conclusive decision was reached. Any vessels that did not achieve agreement by discussion were excluded from the analysis.

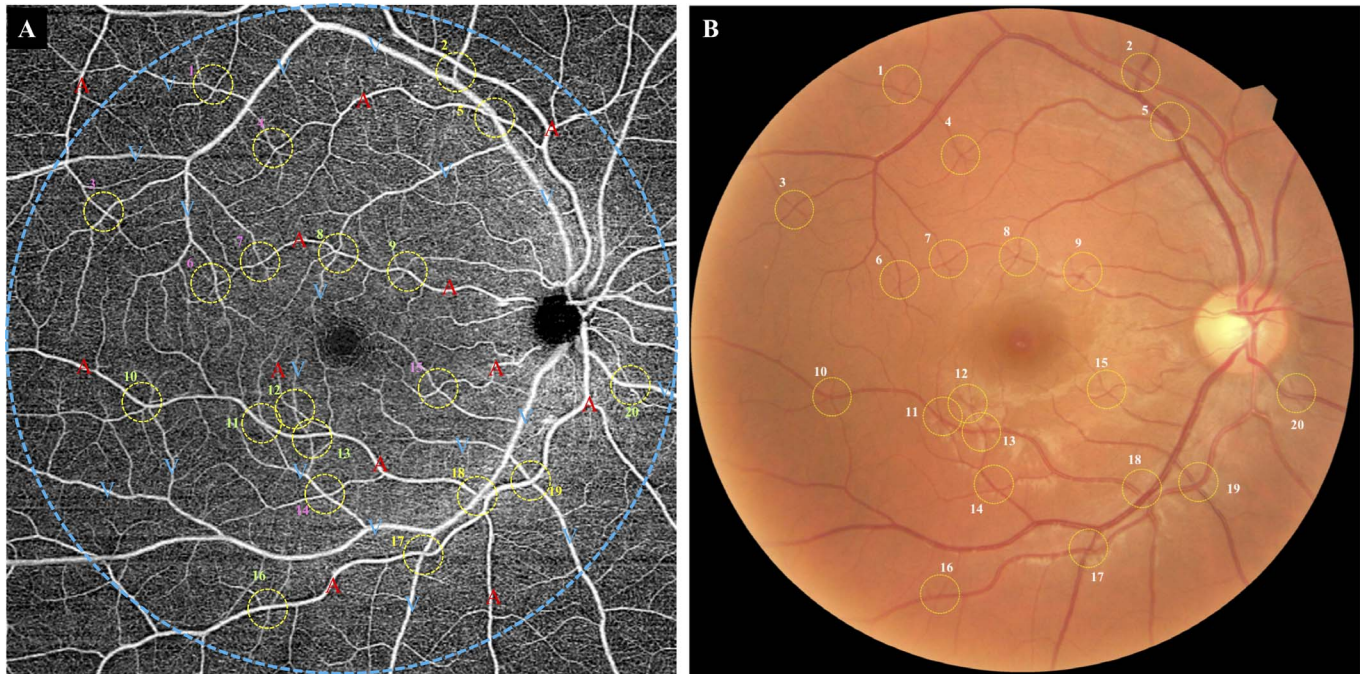


**Figure 2.** Evaluated arteriovenous crossing in the en face OCTA image (A) and the CFP (B) of the same normal eye as in Figure 1. (A) After grading of arteries and veins using the en face OCTA images, the answers are disclosed: *red A* for arteries, and *blue V* for veins. The *blue-dot circle* represents the area covered by the CFP. Evaluated crossing sites (*yellow circles*) are defined as those in which the vessels are perfectly focused in the CFP (B). The crossing sites are categorized as a large (first- or second-order) vessel versus large vessel (L versus L, *yellow numbers*), a large vessel versus a small (third-order) vessel (L versus S, *green numbers*), or a small vessel versus a small vessel (S versus S, *pink numbers*). The independent masked readers evaluated whether the artery or vein is anterior at the crossing sites (*yellow circles*) using en face OCTA alone. (B) A high-resolution CFP used for making the gold standard crossing determination.

## Identification of Vessel Crossings

The second part of the study focused on evaluation of whether the artery or the vein was anterior at the site of crossing of two vessels. In this grading, the readers were unmasked as to which vessels were arteries and which were veins based on the gold standard. The readers then evaluated whether the artery or vein was anterior at sites of vessel crossing (Fig. 2A). Evaluated crossing sites were chosen for their excellent focus on the high-resolution CFP, providing optimal conditions for gold standard determination of vascular position at the crossing by the two retinal specialists (Fig. 2B). When discrepancies occurred between the retinal specialists, they were openly discussed and a conclusive decision reached. Any crossings that did not achieve agreement by discussion were excluded from the analysis. Crossings were categorized as large (first- or second-order) vessel versus large vessel (L versus L), large vessel versus a small (third-order) vessel (L versus S), or a small vessel versus a small vessel (S versus S).

## Data Analysis

The accuracy in each reader's grading of the OCTA images compared to the gold standard was calculated by the following formula: Accuracy = [(Number of correct answers)/(Number of vessels analyzed)] × 100%. To assess reliability between the graders, Cohen's  $\kappa$  was calculated. All data analyses were performed using statistical software (SPSS v25; SPSS, Inc., Chicago, IL) across four vessel groups (all, first-, second-, and third-order vessels) and three vessel crossing groups (L versus L, L versus S, and S versus S).

## Results

### Baseline Characteristics

For normal subjects, 10 randomly chosen eyes (five right, five left) from 10 healthy volunteers (six male, four female) were analyzed. The mean age was 31 years (range: 25–38 years). We also included 12 eyes (eight right, four left) from nine diabetic patients (six

**Table 1.** Accuracy and Reliability of Artery-Vein Differentiation in Normal Eyes

	Accuracy of Reader 1, %	Accuracy of Reader 2, %	Average Accuracy, %	Cohen's $\kappa$ Between Readers
Total (538 vessels)	99.44 (3 errors)	97.77 (11 errors)	98.61	0.948
First order (119 vessels)	100	98.32 (2 errors)	99.16	0.967
Second order (110 vessels)	100	100	100	1.00
Third order (309 vessels)	99.03 (3 errors)	97.09 (9 errors)	98.06	0.920

male, three female). The mean age of the patients in the diabetic group was 53 years (range: 34–73 years). Four eyes were diagnosed as severe nonproliferative DR (NPDR), and eight eyes as proliferative DR (PDR). The mean number of vessels evaluated in each image was 53 vessels (range: 46–61 vessels) for each normal eye and 54 vessels (range: 48–66 vessels) for each diabetic eye.

### Artery-Vein Identification in Normal Eyes

A total of 539 vessels were evaluated in normal eyes. In determining the gold standard from CFP, eight discrepancies in third-order vessels arose between the two retinal specialists (Cohen's  $\kappa = 0.970$ ). Seven of them were conclusively decided by open

discussion, but one could not be conclusively determined and was excluded. Therefore, 538 vessels were used for the final analysis. The number of first-, second-, and third-order vessels were 119, 110, and 309, respectively.

The accuracy of readers 1 and 2 and the reliability between readers are shown in Table 1. The average accuracies in identifying all, first-, second-, and third-order vessels were 98.61%, 99.16%, 100%, and 98.06%, respectively. Cohen's  $\kappa$  between graders for all, first-, second-, and third-order vessels was 0.948, 0.967, 1.00, and 0.920, respectively. Notably, both readers perfectly identified second-order vessels (Fig. 3). Reader 2 misread two first-order vessels on the nasal side (Fig. 4). In the macular region, the third-

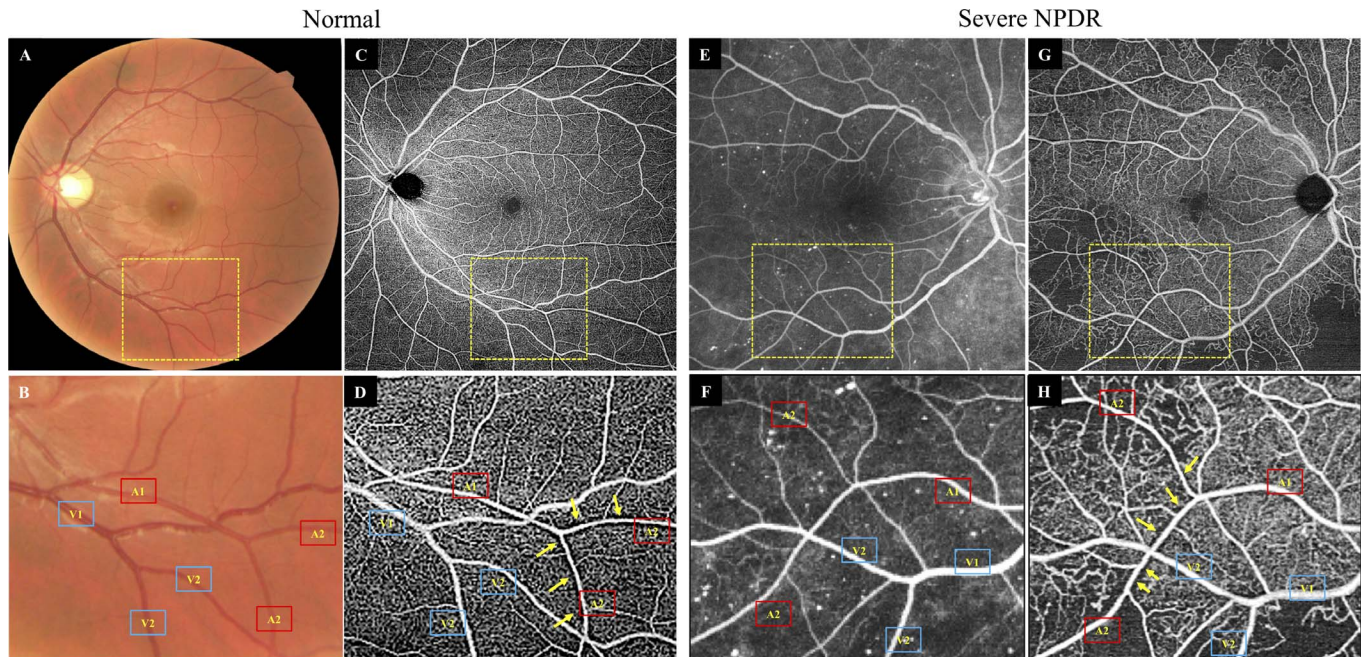


**Figure 3.** Clear identification of first- and second-order arteries and veins on OCTA images of a normal (A–D) and a severe NPDR eye (E–H). Yellow rectangles in the upper row are magnified in the bottom row. A1 and V1 represent a first-order artery and vein, respectively. A2 and V2 are a second-order artery and vein, respectively. (A, B) CFP of a healthy left eye (25-year-old male). (C, D) OCTA images,  $12 \times 12$  mm, of the same normal eye clearly show periarterial capillary-free zones (yellow arrows), especially around the second-order arteries. (E, F) FA images of a right eye with severe NPDR (59-year-old male). (G, H) OCTA images,  $12 \times 12$  mm, of the same diabetic eye also show periarterial capillary-free zones (yellow arrows), especially around the second-order arteries.

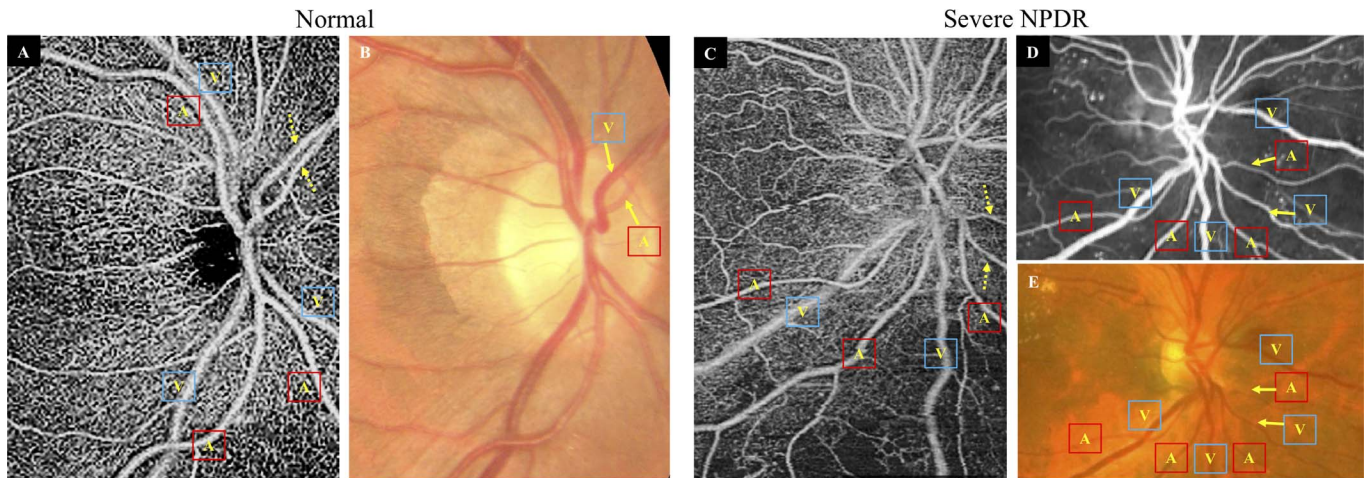


**Figure 4.** Difficult cases in identifying first-order arteries and veins on the nasal side of OCTA images. A and V represent arteries and veins, respectively. (A) The magnified  $12 \times 12$ -mm OCTA image at the disc of a normal right eye (34-year-old male). Temporal arteries and veins are easily differentiated, but the nasal ones are challenging (yellow-dot arrows). (B) The magnified CFP at the disc of the same area as (A). CFP reveals the nasal artery and vein (yellow arrows). (C) Magnified  $12 \times 12$ -mm OCTA image at the disc of the right eye with severe NPDR (73-year-old male). It is similarly difficult to differentiate the nasal vessels (yellow-dot arrows). (D) FA and CFP (E) taken with Optos California can easily identify the nasal arteries and veins (yellow arrows).

order vessels that overlapped or intertwined with each other were also sometimes misread (Fig. 5).

### Artery-Vein Identification in Diabetic Eyes

A total of 649 vessels were evaluated in diabetic eyes. In determining the gold standard from CFP and FA, there were 11 discrepancies between the two retinal specialists in identification of third-order vessels (Cohen's  $\kappa = 0.966$ ). Two vessels were regarded as IRMAs and thus were excluded. Seven vessels were conclusively decided by open discussion, but two were not and were also excluded. Therefore, 645 vessels were used for the final analysis. The numbers of first-, second-, third-order vessels were 184, 159, and 302, respectively.

The accuracies of readers 1 and 2 and the reliability between readers are shown in Table 2. The average accuracies identifying all, first-, second-, and third-order vessels were 96.90%, 99.46%, 97.77%, and 94.85%, respectively. Cohen's  $\kappa$  between graders

for all, first-, second-, and third-order vessels was 0.888, 0.978, 0.935, and 0.808, respectively. First- and second-order vessels were almost perfectly identified by both readers. However, reader 2 misread two first-order vessels on the nasal side in a fashion similar to the normal case (Fig. 4). However, in contrast to the normal case, some misreading occurred even in the second-order vessels (Fig. 6). Third-order vessels in diabetic eyes were less accurately and reliably identified than those in the normal eyes (Fig. 5 and 6).

### Crossing Identification

A total of 170 crossings from the 10 normal eyes were evaluated. In determining the gold standard from CFP, eight discrepancies were found between the results from the two retinal specialists (Cohen's  $\kappa = 0.906$ ). Six of them were conclusively decided by open discussion, but two were not and were excluded. Therefore, 168 crossings were used for the final

**Table 2.** Accuracy and Reliability of Artery-Vein Differentiation in Diabetic Eyes

	Accuracy of Reader 1, %	Accuracy of Reader 2, %	Average Accuracy, %	Cohen's $\kappa$ Between Readers
Total (645 vessels)	98.91 (7 errors)	94.88 (33 errors)	96.90	0.888
First order (184 vessels)	100	98.91 (2 errors)	99.46	0.978
Second order (159 vessels)	98.74 (2 errors)	96.80 (5 errors)	97.77	0.935
Third order (302 vessels)	98.34 (5 errors)	91.36 (26 errors)	94.85	0.808

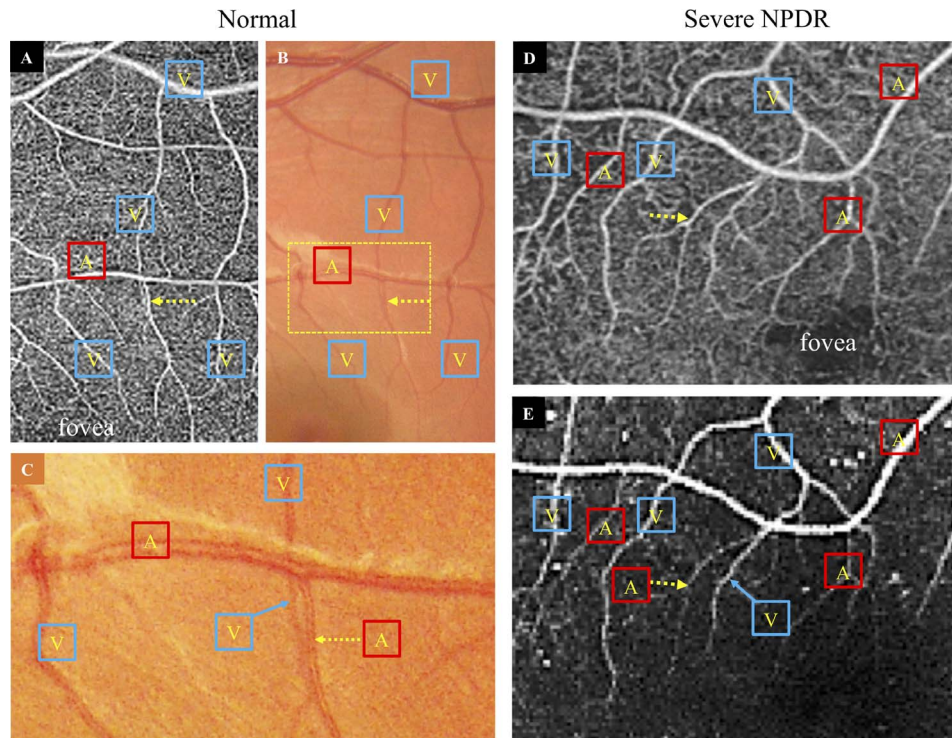


**Figure 5.** Difficult cases in identifying third-order arteries and veins on OCTA images of a normal (A–C) and a severe NPDR eye (D, E). A and V represent arteries and veins, respectively. (A) The magnified  $12 \times 12$ -mm OCTA image of the normal left eye (25-year-old male). The *yellow-dot arrow* shows a third-order vessel that appears to be continuous with the more superior vertically oriented vein. (B, C) The CFP of the same eye as in A. (C) shows the magnified area from the *yellow rectangle* in (B). The *blue arrow* indicates another vein that is blocked from view in the OCTA image but clearly is actually the vessel continuous with the upper vein. Therefore, the vessel indicated by the *yellow-dot arrow* in A and B is actually an artery. (D) The magnified  $12 \times 12$ -mm OCTA image of a right eye with severe NPDR (59-year-old male). The vessel indicated by the *yellow-dot arrow* appears intertwined with another proximal vessel. (E) However, the FA image clearly shows that the other vessel (*blue arrow*) is continuous with the upper vein; therefore, the vessel shown as a *yellow-dot arrow* is an artery.

analysis. The number of L versus L, L versus S, and S versus S crossings were 54, 76, and 38, respectively.

The accuracies of readers 1 and 2 and the reliability between readers are shown in [Table 3](#). The average accuracies with respect to the gold standard, to which the two readers were blinded, in identifying all, L versus L, L versus S, and S versus S crossings were 60.71%, 87.97%, 40.79%, and 61.85%, and Cohen's  $\kappa$  for the same groups was 0.659, 0.783,

0.546, and 0.632, respectively ([Table 3](#)). Compared to artery-vein identification, the accuracy and reliability were low even in L versus L crossings. Reverse visualization of relative vessel depth at crossing sites frequently occurred on the en face OCTA with respect to the gold standard, especially at L versus S crossings ([Fig. 7](#)). However, following and tracing flow signals on flow-overlaid B-scans could reveal which vessel was truly anterior ([Fig. 7C, F, and I](#)).

**Table 3.** Accuracy and Reliability of Arteriovenous Crossing Identification in Normal Eyes

	Accuracy of Reader 1, %	Accuracy of Reader 2, %	Average Accuracy, %	Cohen's $\kappa$ Between Readers
Total (168 crossings)	60.11 (67 errors)	61.31 (65 errors)	60.71	0.659
L vs. L (54 crossings)	85.19 (8 errors)	90.74 (5 errors)	87.97	0.783
L vs. S (76 crossings)	40.79 (45 errors)	40.79 (45 errors)	40.79	0.546
S vs. S (38 crossings)	63.16 (14 errors)	60.53 (15 errors)	61.85	0.632

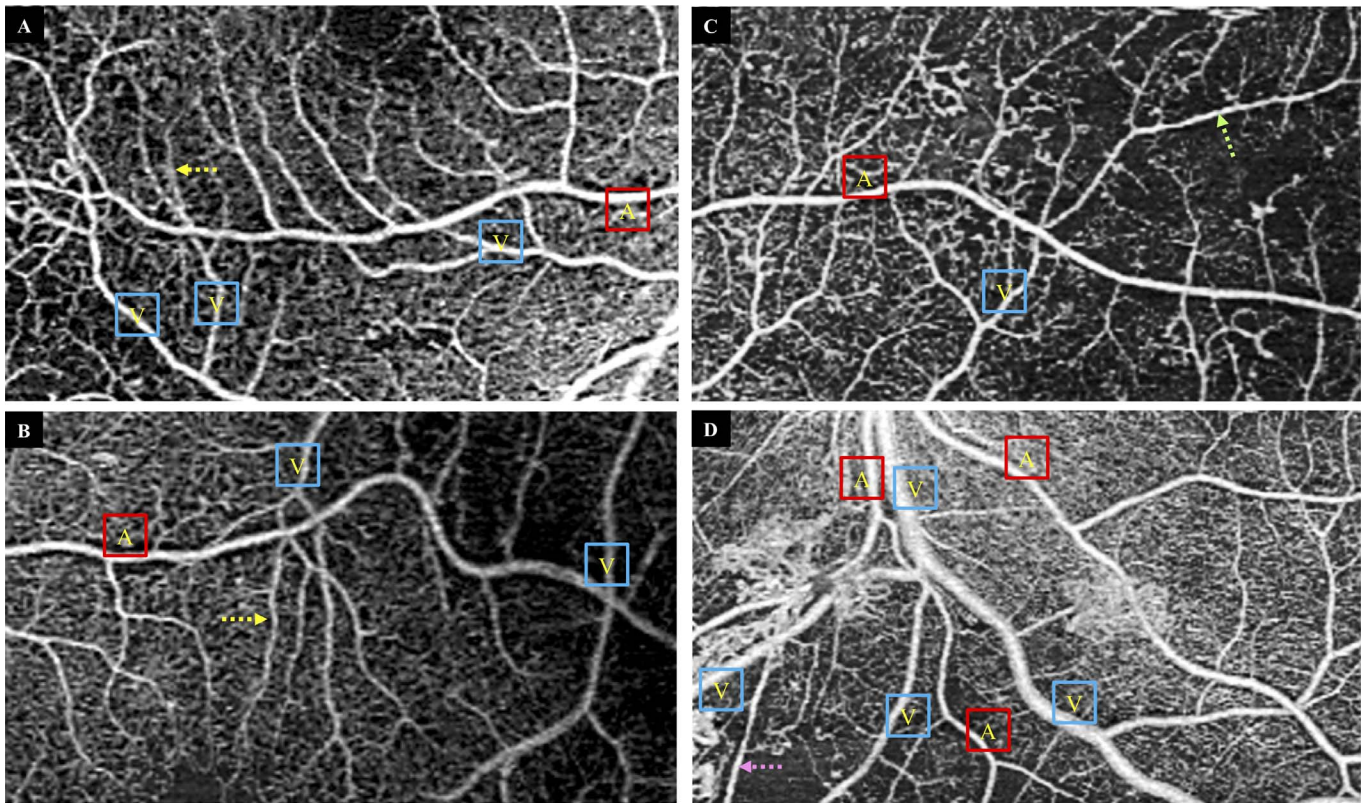


**Figure 6.** Difficult diabetic cases in differentiating arteries and veins on OCTA. A and V represent arteries and veins, respectively. (A) A right eye with PDR (37-year-old female). (B) A left eye with PDR (73-year-old male). The vessels indicated by the *yellow-dot arrows* in (A) and (B) appear to be veins, but they are intertwined with another vessel. Moreover, small capillary dropout around the vessels makes the periarterial capillary-free zones difficult to discern. (C, D) OCTA images of a left eye with PDR (62-year-old male). At the temporal area (C), capillary dropout and abnormalities are more severe than in (A) and (B). The vessel indicated by the *green-dot arrow* appears to be an artery but is difficult to conclusively identify on OCTA alone. At the inferior nasal area (D), projection of neovascular tissues is covering over the proximal large vessels. The second-order vessel indicated by the *pink arrow* appears to be an artery, but the neovascular projections interfere with identifying its proximal connection.

## Discussion

A recent study, which developed automatic artery-vein differentiation in  $6 \times 6$ -mm OCTA guided by color fundus images from normal and diabetic subjects, demonstrated more than 98% accuracy in identifying vessels as arteries and veins.<sup>21</sup> Our study investigated the accuracy and reliability in manually differentiating retinal arteries and veins using only  $12 \times 12$ -mm en face OCTA images in normal eyes and eyes with severe DR. The overall accuracies of the readers were high in normal eyes ( $>97\%$ ) and still relatively high in diabetic eyes ( $>94\%$ ). For first- and second-order vessels, OCTA enables identification of arteries and veins almost perfectly in normal eyes (accuracy:  $>98\%$ , Cohen's  $\kappa$ :  $>0.96$ ) and even in diabetic eyes (accuracy:  $>96\%$ , Cohen's  $\kappa$ :  $>0.93$ ). Our results suggest that readers can correctly identify

the large arteries and veins using only widefield OCTA if they are taught how to differentiate arteries from veins on OCTA using the aforementioned rules. Moreover, widefield OCTA images have adequate resolution to visualize third-order vessels, which can be accurately identified, presumably by tracing these vessels back to easily identified second-order vessels and making use of the fact that physiologically like vessels do not cross like (i.e., artery-artery, vein-vein). Third-order vessels also were accurately classified with an average accuracy above 90%, even in the diabetic eyes.

The most notable result of the current study was that second-order vessels in normal eyes were perfectly identified by both readers (Table 1). This could be explained by the fact that the capillary-free zone is quite visible around the second-order branches of the retinal arteries in OCTA images (Fig. 3). Michaelson and Campbell<sup>24</sup> for the first time showed

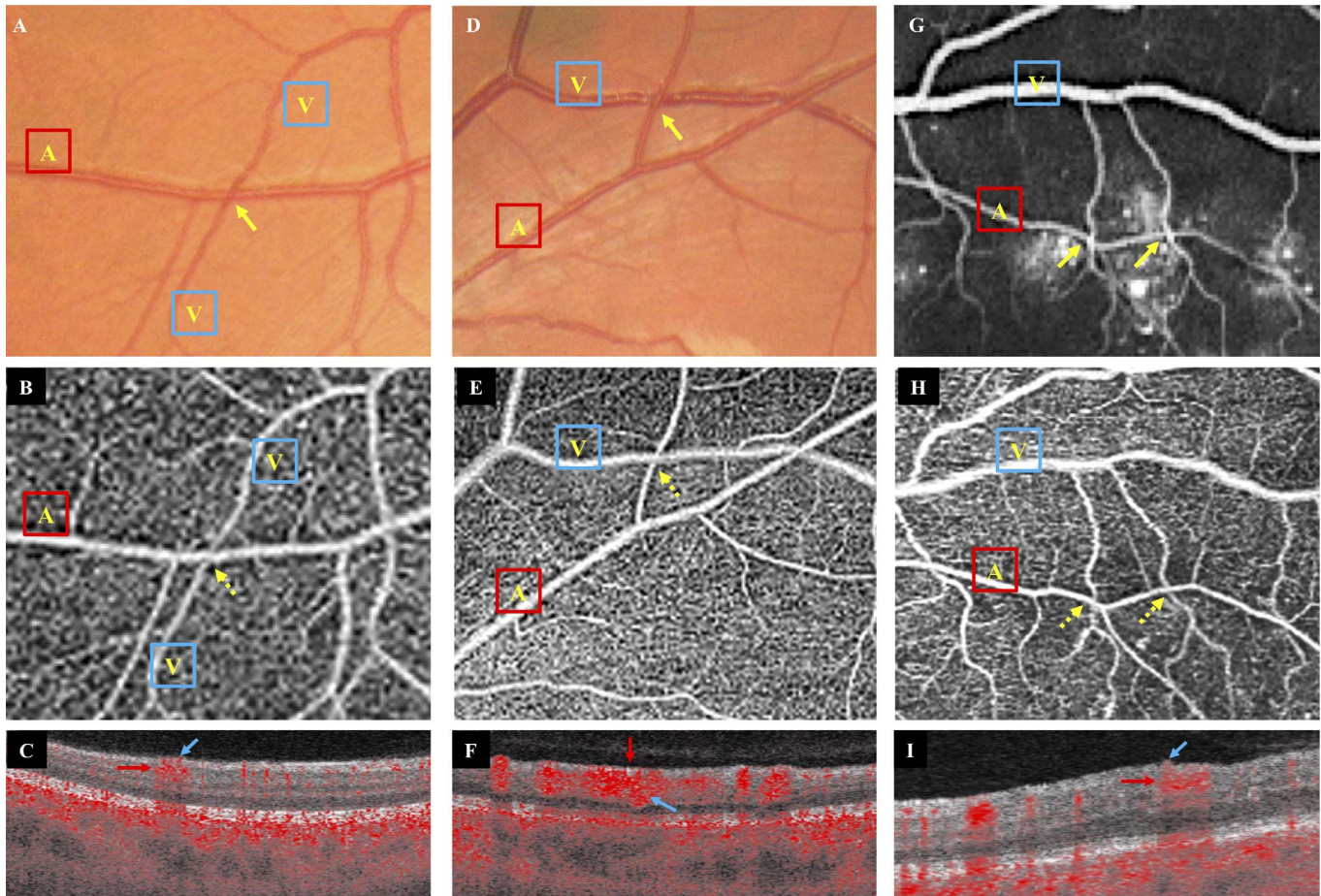


**Figure 7.** Typical cases representing the “crossing artifact.” A and V represent arteries and veins, respectively. (A) Magnified CFP of a normal right eye (34-year-old male). A *yellow arrow* shows a third-order vein crossing over a second-order artery. (B) The corresponding OCTA image to (A) displays the large artery as overlaying the small vein, reversing the actual depth order of the vessels (*dot arrows*). (C) Horizontal flow-overlaid OCT B-scan at the crossing site in (B) (*yellow-dot arrow*) shows that the vein (*blue arrow*) is actually crossing over the artery (*red arrow*). (D) Magnified CFP of the normal left eye (25-year-old male). *Arrows* show second-order artery crossing over a second-order vein. (E) The corresponding OCTA image to (D) displays the vein as inversely overlaying the artery (*yellow-dot arrow*). (F) Horizontal flow-overlaid OCT B-scan at the crossing site in (E) (*yellow-dot arrow*) shows that the artery (*red arrow*) is actually crossing over the vein (*blue arrow*). (G) Magnified FA image of a left eye with severe NPDR (73-year-old male). *Arrows* show third-order veins crossing over a second-order artery. (H) The corresponding OCTA image to (E) displays the large artery as overlaying the small veins. (I) Horizontal flow-overlaid OCT B-scan at the crossing site on H (*right yellow-dot arrow*) shows that the vein (*blue arrow*) is actually crossing over the artery (*red arrow*).

histologically the presence of a capillary-free zone along human retinal arteries. The capillary-free zone develops during embryogenesis because transmurial oxygen diffusion is capable of satisfying the metabolic demands of the cells immediately adjacent to the retinal artery, mitigating the need for vessels in this area.<sup>24</sup> Thus, the periarterial capillary-free zone is an area of physiological avascularization. Recently, Balaratnasingam<sup>22</sup> demonstrated the prominent capillary-free zone along the retinal artery in OCTA slabs containing the superficial plexus and all capillary plexuses using four different devices, including the

PLEX Elite 9000. When the second-order arteries are identified according to the capillary-free zone, they can also be traced proximally and distally to identify first- and third-order arteries. Therefore, the periarterial capillary-free zone is among the most important characteristics in differentiating arteries from veins using only OCTA.

It is interesting that identification of the first-order vessels was not perfect for both readers, and all misreading of first-order vessels occurred near the nasal side of the optic disc (Fig. 4). On 12 × 12-mm OCTA images centered on the fovea, second-order

vessels are not always included in the scan area. Thus, the readers cannot trace back from the second-order arteries that have the abovementioned prominent capillary-free zone. Furthermore, it has been reported that the proximal part of the first-order retinal arteries around the optic disc have a narrower capillary-free zone than do second-order arterial branches.<sup>25</sup> Also, dense radial peripapillary capillaries in this area make the periarterial capillary-free zone of the proximal retinal arteries blurred. Misreading of first-order vessels on OCTA images could potentially be avoided if the nasal side is scanned as well when generating widefield montage images.<sup>26</sup>

The accuracy and reliability in identifying third-order vessels was less than for first- and second-order vessels (Tables 1 and 2). However, as demonstrated by the relatively high Cohen's  $\kappa$  in normal (0.920) and diabetic eyes (0.808), the misreading occurred in similar vessels that were difficult for both readers to identify (Figs. 5 and 6). Overlapping and intertwined vessels sometimes lead to misreading partly because the resolution in  $12 \times 12$ -mm OCTA images is not sufficient to visualize vessels closely located to each other. Increased resolution in widefield OCTA images could overcome this problem. Furthermore, third-order arteries and veins become, more distally, precapillary arterioles and venules in order to supply and drain the retinal tissues. At the level of these small-size vessels, arterioles are physiologically next to venules in order to facilitate efficient metabolic exchange; this alternating distribution of the arterioles and venules has been three-dimensionally reported in the histology of mice and pig retinas<sup>27,28</sup> and using OCTA devices in human retinas.<sup>29</sup> Using this heuristic, looking at the neighboring third-order arteries and veins is sometimes helpful in identifying intertwined vessels as either arterial or venous (Fig. 5).

In severe diabetic cases, however, the alternation of arterioles and venules can be violated due to capillary occlusion and dropout. As a number of studies have demonstrated, capillary density significantly decreases in eyes with severe DR as compared to normal, no DR, or mild DR cases.<sup>30–35</sup> Decreased capillary density would make the periarterial capillary-free zone more difficult to discern (Fig. 6). Furthermore, from histological studies, the non-perfusion areas in DR are known to be more likely located adjacent to arterioles,<sup>36,37</sup> which could further confound the utility of the capillary-free zone in identifying arteries. In cases of PDR, the presence of NVE also adds difficulty to accurately identifying

vessels, as projection of the NVE interface can obscure the view of vessel connections. In our study, the individual reader accuracy and the reliability between readers was lower in the diabetic eyes as compared to normal eyes (Table 2). This suggests that when identifying vessels in diabetic eyes, it is important to use CFP and FA in combination with OCTA rather than relying on en face OCTA alone.

Although in general the results of artery-vein identification suggest that arteries and veins can be identified with a relatively high degree of accuracy and reliability using en face OCTA alone, this was not the case for all areas of the image and was especially not the case for the arteriovenous crossing sites (Table 3). When analyzing the crossing features, it was noted that en face OCTA did not accurately depict the relative depth of vessels as compared to CFP or CFP and FA, resulting in a “crossing artifact” (Fig. 7). For example, where a small vein was known from CFP and/or FA to cross over a large artery, en face OCTA images in this data set often displayed the large artery as overlaying the small vein—reversing the actual depth order of the vessels. In crossings between large vessels, reverse visualization of this kind was rare, but still occurred. In these cases, referring to the OCT B-scans with flow overlay revealed which vessel was actually anterior (Fig. 7); identifying arteriovenous crossing using OCT B-scans has been demonstrated in eyes with branch RVO.<sup>38,39</sup> A previous study focusing on venous nicking without arteriovenous contact using adaptive optics images showed that the various ophthalmoscopic presentations of arteriovenous nickings might result from the combined effects of hypertrophy and retraction of the intervacular space.<sup>40</sup> Initially, we were not sure if the crossing artifact was related to the microenvironment surrounding small arteries and venules. However, we confirmed that this finding was inconsistent across different OCTA devices and imaging sizes (Supplemental Fig. S2), suggesting that this crossing artifact may be a function of each device's processing algorithms for constructing the en face OCTA image. Therefore, when determining which vessel is anterior at crossing points in OCTA images, it is important to use CFP and FA in combination with flow-overlaid OCT B-scans, rather than relying on en face OCTA alone.

In contrast to the CFP and FA, OCTA is neither widely available for all clinicians nor the gold standard in differentiating arteries from veins in daily clinical practice. However, if available, OCTA allows for easy assessment of not only precapillary arterial

and venous changes but also capillary-level alterations. The current results could contribute to direct observation of the arterial-side or venous-side microvascular changes in the retinal diseases and the estimation of their pathogenesis. Furthermore, the presence of leakage in eyes with DR on FA reinforces that en face OCTA can serve as a “clean” imaging modality that shows no leakage, making differentiation of arteries and veins easier. In addition, the current analyses may also apply to machine learning and automated interpretation of the OCTA images. Further studies assessing the roles of these new technologies are needed.

This study had several limitations. First, only normal and diabetic eyes were included. The effects of other pathologies, such as branch RVO, on artery-vein differentiation could be different and require further investigation. Second, eyes with minor media opacity or pseudophakia were included. As opposed to FA, OCTA images do not have “phase” information; thus, it might be difficult to identify arteries and veins in low-quality OCTA images due to severe media opacity. The selection bias of so-called perfect-to-image eyes is a limitation of the current study. Third, our study was limited to 12 × 12-mm images. The accuracy of vessel identification using other image sizes that capture both first- and second-order vessels, such as 6 × 6 mm, is unclear. The vessels captured in 3 × 3-mm scans are mostly third-order or precapillary arterioles and venules, so accurate identification using the methodology described in this study would be challenging. Finally, this study included only images obtained using the Carl Zeiss PLEX Elite 9000. Further investigation is needed to fully understand the accuracy and reliability of vessel and crossing identification using other devices, including spectral-domain OCTA devices. This is particularly important given the impact that variable processing algorithms can have on how vessel information is displayed in en face OCTA images.

In conclusion, OCTA images allow for overall accurate and reliable artery and vein identification; however, for small branches and at areas of vessel crossing, identification by OCTA alone may be less accurate and reliable.

## Acknowledgments

Disclosure: **A. Ishibazawa**, Grant-in-Aid for Scientific Research, 19K09925 (F); **N. Mehta**, None; **O. Sorour**, None; **P. Braun**, Yale Medical Student

Research Fellowship (F); **S. Martin**, None; **A.Y. Alibhai**, None; **A. Saifuddin**, None; **M. Arya**, None; **C.R. Baumal**, Genentech (C); **J.S. Duker**, Carl Zeiss Meditec, Inc., Optovue, Inc., Topcon Medical Systems, Inc., Novartis Phama AG., Roche (F), Carl Zeiss Meditec, Inc., Optovue, Inc., Topcon Medical Systems, Inc. (C); **N.K. Waheed**, Macula Vision Research Foundation, Carl Zeiss Meditec, Inc., Optovue, Inc., Topcon Medical Systems, Inc., Nidek Medical Products, Inc. (F), Optovue, Inc., Regeneration, Genentech (C)

## References

1. Keith NM, Wagener HP, Barker NW. Some different types of essential hypertension: their course and prognosis. *Am J Med Sci.* 1974;268:336–345.
2. Klein R, Klein BE, Moss SE, Wang Q. Hypertension and retinopathy, arteriolar narrowing, and arteriovenous nicking in a population. *Arch Ophthalmol.* 1994;112:92–98.
3. Klein R, Sharrett AR, Klein BE, et al. Are retinal arteriolar abnormalities related to atherosclerosis?: the Atherosclerosis Risk in Communities Study. *Arterioscler Thromb Vasc Biol.* 2000;20:1644–1650.
4. Early Treatment Diabetic Retinopathy Study Research Group. Grading diabetic retinopathy from stereoscopic color fundus photographs—an extension of the modified Airlie House classification. ETDRS report number 10. *Ophthalmology.* 1991;98:786–806.
5. Wilkinson CP, Ferris FL III, Klein RE, et al. Proposed international clinical diabetic retinopathy and diabetic macular edema disease severity scales. *Ophthalmology.* 2003;110:1677–1682.
6. Fonseca RA, Dantas MA. Retinal venous beading associated with recurrent branch vein occlusion. *Can J Ophthalmol.* 2002;37:182–183.
7. Sharrett AR, Hubbard LD, Cooper LS, et al. Retinal arteriolar diameters and elevated blood pressure: the Atherosclerosis Risk in Communities Study. *Am J Epidemiol.* 1999;150:263–270.
8. Hubbard LD, Brothers RJ, King WN, et al. Methods for evaluation of retinal microvascular abnormalities associated with hypertension/sclerosis in the Atherosclerosis Risk in Communities Study. *Ophthalmology.* 1999;106:2269–2280.
9. Ikram MK, Janssen JA, Roos AM, et al. Retinal vessel diameters and risk of impaired fasting

- glucose or diabetes: the Rotterdam study. *Diabetes*. 2006;55:506–510.
10. Ikram MK, Witteman JC, Vingerling JR, Breteler MM, Hofman A, de Jong PT. Retinal vessel diameters and risk of hypertension: the Rotterdam Study. *Hypertension*. 2006;47:189–194.
  11. Kawasaki R, Cheung N, Wang JJ, et al. Retinal vessel diameters and risk of hypertension: the Multiethnic Study of Atherosclerosis. *J Hypertens*. 2009;27:2386–2393.
  12. Hanssen H, Nickel T, Drexel V, et al. Exercise-induced alterations of retinal vessel diameters and cardiovascular risk reduction in obesity. *Atherosclerosis*. 2011;216:433–439.
  13. Zhu P, Huang F, Lin F, et al. The relationship of retinal vessel diameters and fractal dimensions with blood pressure and cardiovascular risk factors. *PLoS One*. 2014;9:e106551.
  14. Kashani AH, Chen CL, Gahm JK, et al. Optical coherence tomography angiography: a comprehensive review of current methods and clinical applications. *Prog Retin Eye Res*. 2017;60:66–100.
  15. Spaide RF, Fujimoto JG, Waheed NK, Sadda SR, Staurengi G. Optical coherence tomography angiography. *Prog Retin Eye Res*. 2018;64:1–55.
  16. Sridhar J, Shahlaee A, Rahimy E, et al. Optical coherence tomography angiography and en face optical coherence tomography features of paracentral acute middle maculopathy. *Am J Ophthalmol*. 2015;160:1259–1268.e2.
  17. Iafe NA, Onclinx T, Tsui I, Sarraf D. Paracentral acute middle maculopathy and deep retinal capillary plexus infarction secondary to reperfused central retinal artery occlusion. *Retin Cases Brief Rep*. 2017;11(suppl 1):S90–S93.
  18. Ghasemi Falavarjani K, Phasukkijwatana N, Freund KB, et al. En face optical coherence tomography analysis to assess the spectrum of perivenular ischemia and paracentral acute middle maculopathy in retinal vein occlusion. *Am J Ophthalmol*. 2017;177:131–138.
  19. Pan J, Chen D, Yang X, et al. Characteristics of neovascularization in early stages of proliferative diabetic retinopathy by optical coherence tomography angiography. *Am J Ophthalmol*. 2018;192:146–156.
  20. Freund KB, Sarraf D, Leong BCS, Garrity ST, Vupparaboina KK, Dansingani KK. Association of optical coherence tomography angiography of collaterals in retinal vein occlusion with major venous outflow through the deep vascular complex. *JAMA Ophthalmol*. 2018;136:1262–1270.
  21. Alam M, Toslak D, Lim JI, Yao X. Color fundus image guided artery-vein differentiation in optical coherence tomography angiography. *Invest Ophthalmol Vis Sci*. 2018;59:4953–4962.
  22. Balaratnasingam C, An D, Sakurada Y, et al. Comparisons between histology and optical coherence tomography angiography of the periarterial capillary-free zone. *Am J Ophthalmol*. 2018;189:55–64.
  23. Muraoka Y, Uji A, Ishikura M, Iida Y, Ooto S, Tsujikawa A. Segmentation of the four-layered retinal vasculature using high-resolution optical coherence tomography angiography reveals the microcirculation unit. *Invest Ophthalmol Vis Sci*. 2018;59:5847–5853.
  24. Michaelson I, Campbell A. The anatomy of the finer retinal vessels, and some observations on their significance in certain retinal diseases. *Trans Ophthalmol Soc UK*. 1940;60:71–111.
  25. Mase T, Ishibazawa A, Nagaoka T, Yokota H, Yoshida A. Radial peripapillary capillary network visualized using wide-field montage optical coherence tomography angiography. *Invest Ophthalmol Vis Sci*. 2016;57:OCT504–510.
  26. Sawada O, Ichiyama Y, Obata S, et al. Comparison between wide-angle OCT angiography and ultra-wide field fluorescein angiography for detecting non-perfusion areas and retinal neovascularization in eyes with diabetic retinopathy. *Graefes Arch Clin Exp Ophthalmol*. 2018;256:1275–1280.
  27. Paques M, Tadayoni R, Sercombe R, et al. Structural and hemodynamic analysis of the mouse retinal microcirculation. *Invest Ophthalmol Vis Sci*. 2003;44:4960–4967.
  28. Fouquet S, Vacca O, Sennlaub F, Paques M. The 3D retinal capillary circulation in pigs reveals a predominant serial organization. *Invest Ophthalmol Vis Sci*. 2017;58:5754–5763.
  29. Bonnin S, Mane V, Couturier A, et al. New insight into the macular deep vascular plexus imaged by optical coherence tomography angiography. *Retina*. 2015;35:2347–2352.
  30. Agemy SA, Scripsema NK, Shah CM, et al. Retinal vascular perfusion density mapping using optical coherence tomography angiography in normals and diabetic retinopathy patients. *Retina*. 2015;35:2353–2363.
  31. Kim AY, Chu Z, Shahidzadeh A, Wang RK, Puliafito CA, Kashani AH. Quantifying microvascular density and morphology in diabetic retinopathy using spectral-domain optical coherence tomography angiography. *Invest Ophthalmol Vis Sci*. 2016;57:OCT362–370.
  32. Kaizu Y, Nakao S, Yoshida S, et al. Optical coherence tomography angiography reveals spa-

- tial bias of macular capillary dropout in diabetic retinopathy. *Invest Ophthalmol Vis Sci.* 2017;58:4889–4897.
33. Ting DSW, Tan GSW, Agrawal R, et al. Optical coherence tomographic angiography in type 2 diabetes and diabetic retinopathy. *JAMA Ophthalmol.* 2017;135:306–312.
  34. Hirano T, Kitahara J, Toriyama Y, Kasamatsu H, Murata T, Sadda S. Quantifying vascular density and morphology using different swept-source optical coherence tomography angiographic scan patterns in diabetic retinopathy [published online ahead of print April 29, 2018]. *Br J Ophthalmol*.doi: 10.1136/bjophthalmol-2018-311942.
  35. Onishi AC, Nesper PL, Roberts PK, et al. Importance of considering the middle capillary plexus on OCT angiography in diabetic retinopathy. *Invest Ophthalmol Vis Sci.* 2018;59:2167–2176.
  36. Ashton N. Arteriolar involvement in diabetic retinopathy. *Br J Ophthalmol.* 1953;37:282–292.
  37. Gardiner TA, Archer DB, Curtis TM, Stitt AW. Arteriolar involvement in the microvascular lesions of diabetic retinopathy: implications for pathogenesis. *Microcirculation.* 2007;14:25–38.
  38. Muraoka Y, Tsujikawa A, Murakami T, et al. Morphologic and functional changes in retinal vessels associated with branch retinal vein occlusion. *Ophthalmology.* 2013;120:91–99.
  39. Iida Y, Muraoka Y, Ooto S, et al. Morphologic and functional retinal vessel changes in branch retinal vein occlusion: an optical coherence tomography angiography study. *Am J Ophthalmol.* 2017;182:168–179.
  40. Paques M, Brolly A, Benesty J, et al. Venous nicking without arteriovenous contact: the role of the arteriolar microenvironment in arteriovenous nickings. *JAMA Ophthalmol.* 2015;133:947–950.